2005

Visible-ultraviolet spectroscopic ellipsometry of lead zirconate titanate thin films

Hosun Lee
Virginia Commonwealth University, hlee@khu.ac.kr

Youn Seon Kang
Virginia Commonwealth University

Sang-Jun Cho
Virginia Commonwealth University

See next page for additional authors

Lee, H., Kang, Y.S., Cho, S.-J., et al. Visible-ultraviolet spectroscopic ellipsometry of lead zirconate titanate thin films. Applied Physics Letters, 86, 262902 (2005).

Visible-ultraviolet spectroscopic ellipsometry of lead zirconate titanate thin films

Hosun Lee,[a] Youn Seon Kang, Sang-Jun Cho, Bo Xiao, and Hadis Morkoç
Department of Electrical Engineering, Virginia Commonwealth University, 601 West Main Street, Richmond, Virginia 23284-9068

Tae Dong Kang
Department of Physics, Kyung Hee University, Suwon 449-701, South Korea

(Received 9 March 2005; accepted 19 May 2005; published online 22 June 2005)

We measured pseudodielectric functions in the visible-ultraviolet spectral range of $Pb(Zr_xTi_{1-x})O_3$ (x=0.2, 0.56, 0.82) (PZT) grown on platinized silicon substrate using the sol-gel method and also on (0001) sapphire using radio frequency sputtering method. Using a parametric optical constant model, we estimated the dielectric functions of the PZT thin films. Taking the second derivative of the fitted layer dielectric functions and using the standard critical point model, we determined the parameters of the critical points. In the second derivative spectra, the lowest bandgap energy peak near 4 eV is fitted as a double peak for annealed PZTs associated with the perovskite phase. As-grown PZTs have mainly pyrochlore phase and the lowest bandgap is fitted as a single peak. We compared the bandgap energies with literature values. © *2005 American Institute of Physics*. [DOI: 10.1063/1.1968432]

Perovskite oxide materials have a very wide range of applications: various sensors, nonvolatile and dynamic random access memories, tunable capacitors for high-frequency microwave applications, electro-optic modulators, infrared detectors, and microelectromechanical systems, to cite a few. Among various perovskite oxide materials, $Pb(Zr_xTi_{1-x})O_3$ (PZT) is the most popular one due to its excellent ferroelectric and piezoelectric material properties, notwithstanding the shortcoming of fatigue.[1]

Electrical properties of PZT have been investigated intensively.[1] However, the optical properties of PZT have been relatively less investigated.[2–4] Spectroscopic ellipsometry (SE) is capable of measuring the dielectric functions of ferroelectric thin films and subsequently can help determine the thickness, microstructure, and electronic band structures. Several ellipsometric investigations have been reported.[3,4] However, their spectral range was limited to the region below and near the lowest bandgap: between 1.5 and 5 eV.

In this work, we measured the pseudodielectric functions of PZTs using SE in the spectral range between 0.8 and 6.5 eV at room temperature. Using the parametric optical constant (POC) model, we estimated the dielectric functions of PZT layers and determined the critical point (CP) parameters performing standard critical point (SCP) model analysis. The bandgap values so determined are consistent with literature values. However, the lowest bandgap structure is resolved as a double peak for perovskite phase in contrast to a single peak in literature.

We grew $Pb(Zr_xTi_{1-x})O_3$ (x=0.56 and 0.82) (abbreviated as PZT56 and PZT82) samples on sapphire (Al_2O_3) using radio frequency magnetron sputtering. We also formed $Pb(Zr_{0.2}Ti_{0.8})O_3$ (abbreviated as PZT20) using a modified sol-gel method on platinized silicon ($Pt/TiO_2/SiO_2/Si$) obtained from Radiant Technologies. The sputtering- and sol-gel-grown PZT samples were annealed at 800 and 650 °C, respectively, to obtain the perovskite phase. The microstructure and crystal orientation were determined by conventional x-ray diffractometry. As-grown PZT samples have mainly the pyrochlore phase with a small portion of the perovskite phase.[5] After annealing, PZT films grown on platinized silicon using the sol-gel method have mainly the (001) perovskite phase, whereas the PZT films grown using the sputtering method have mainly the (111) phase for PZT56 and mainly (110) phase for PZT82. Spectroscopic ellipsometric measurements were performed using a variable-angle spectroscopic ellipsometry (VASE, J. A. Woollam Co.) at angles of incidence of 65°, 70°, 75° using an autoretarder before and after annealing films.

Figure 1 shows the pseudodielectric functions of PZT.

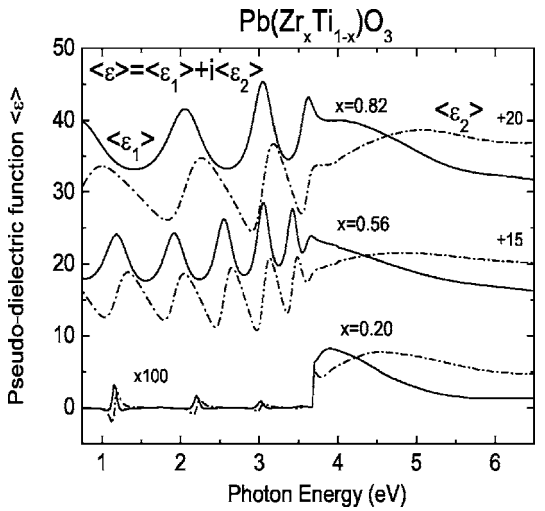

FIG. 1. Pseudo-dielectric functions ($\langle\varepsilon\rangle=\langle\varepsilon_1\rangle+i\langle\varepsilon_2\rangle$) of sol-gel-grown ($x$=0.20) and sputter-grown and annealed (x=0.56 and 0.82) $Pb(Zr_xTi_{1-x})O_3$, in the spectral range of [0.8, 6.5] eV. Real (imaginary) part is designated by solid (dot-dashed) line. The values were shifted for x=0.56 and x=0.82 for convenience.

[a]Permanent address: Department of Physics, Kyung Hee University, Suwon 449-701, S. Korea; electronic mail: hlee@khu.ac.kr

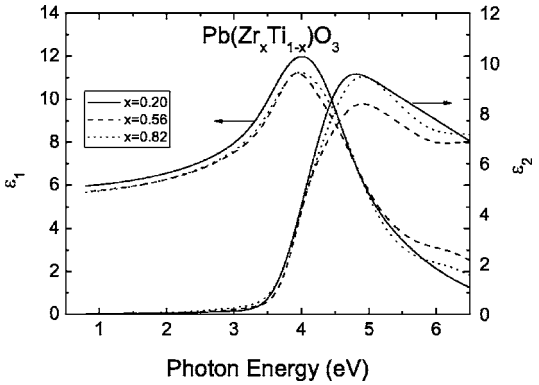

FIG. 2. Fitted dielectric function of annealed PZT layers in the spectral range of [0.8,6.5] eV.

Pseudodielectric functions in the spectral range below 4 eV were dominated by very strong interference patterns for PZT thin films grown on platinized silicon wafers using the sol-gel method, suggesting very abrupt interfaces. In the case of PZTs grown on sapphire substrates with the sputtering method, the interference patterns were not so strong.

We modeled the sample structure consisting of a surface roughness layer, main layer, and substrate. To take into account the surface roughness layer, we used Bruggeman effective medium approximation, assuming the surface roughness layer as a mixture of the main layer and voids.[6] The dielectric function of the main PZT layer was fitted using the POC model. In the POC model, the dielectric function is written as the summation of "*m*" energy-bounded, Gaussian-broadened polynomials and *P* poles accounting for index effects due to absorption outside the model region.[7] Note that we assumed isotropic dielectric functions for PZTs, even though x-ray diffraction data suggested some degree of crystal orientations for different PZTs. The pseudodielectric functions and modeled dielectric functions matched very well and they could not be discerned separately. Surprisingly, the lowest-energy peak of all the PZT films could be fitted as a double peak rather than a single peak using the POC model.

Figure 2 is the fitted dielectric function of each PZT layer. The optical function near 4 eV appears to be composed of a single peak. In literature dealing with the optical properties of PZT films, it has been assumed that the lowest optical structure near 4 eV is a single peak.[3,4] However, the POC model showed that the 4 eV structure of the PZT films have a double peak, as has been corroborated in the second-derivative spectra of the fitted dielectric function shown in Fig. 3(a).

Figure 3(a) is the plot of the second derivative of dielectric functions and their fit using the SCP model. The fitted band-gap energies (E_a and E_b in Fig. 3) are marked with arrows. The SCP model assumes simple parabolic dispersion relation for direct interband transitions.[8] This model provides accurate CP parameters. The SCP line-shape equation is given by, $\varepsilon(\hbar\omega)=C-Ae^{i\Phi}(\hbar\omega-E+i\Gamma)^n$, where the critical point (CP) is described by the amplitude A, threshold energy E, broadening Γ, and the excitonic phase angle Φ. The exponent n has the value $(D-2)/2$ for D-dimensional CPs. Discrete excitons are represented by $n=-1$.

In Fig. 3(a), PZT56 and PZT82 have distinctively double peak structures, probably because sputter-grown PZTs have much higher crystallinity than those grown by sol-gel

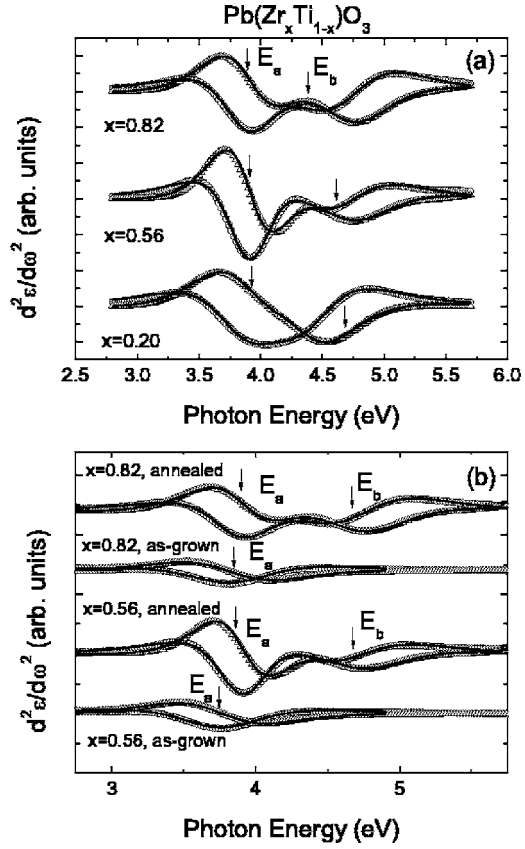

FIG. 3. (a) Plot of second derivative of dielectric functions and their fit for annealed PZTs. The fit bandgap energies E_a and E_b are marked with arrows. (b) Comparison of the second derivative of the dielectric functions PZTs grown on sapphire, as-grown and annealed.

method, according to x-ray diffraction. As shown in Fig. 3(a), we could fit the apparent single peak of PZT20 much better by assuming a double peak rather than a single peak. We found that the exciton peak fit was the best fit for E_a and E_b rather than a 1-, 2-, or 3-dimensional CP fit. The CP, or bandgap, energies were denoted as E_a and E_b for both perovskite and pyrochlore phases in the order of increasing energy for simplicity. Excitonic interaction appears strong in perovskite oxides similar to ZnO. The strong ionic bond character may be responsible for strong excitonic interaction. Actually, perovskite oxide can be classified as a semiconductor because the bandgap is near 4 eV, which is slightly larger than that of ZnO. Here the exciton may be Frenkel rather than Wannier type due to strong localized character.[8]

Figure 3(b) compares the second derivative of the dielectric functions of the as-grown and annealed PZTs (PZT56 and PZT82) grown on sapphire substrates. The as-grown PZT samples show a single peak arising from the pyrochlore phase. The annealed PZT samples show a double peak structure arising from the perovskite structure. Yang *et al.*'s[3] ellipsometry data covered only up to 5 eV and their line-shape fitting using Forouhi-Bloomer model dielectric function gave only single peak, in contrast to our double peak fitting. The x-ray data of annealed PZT samples reported by Yang *et al.* showed significant amount of remaining pyrochlore phase as well as the perovskite phase. This may explain why those authors could fit the optical structure as a single peak rather than as a double peak. Our annealed PZT samples show only the perovskite phase. The lowest bandgap energy E_a of the pyrochlore phase is smaller than that of the perovskite phase

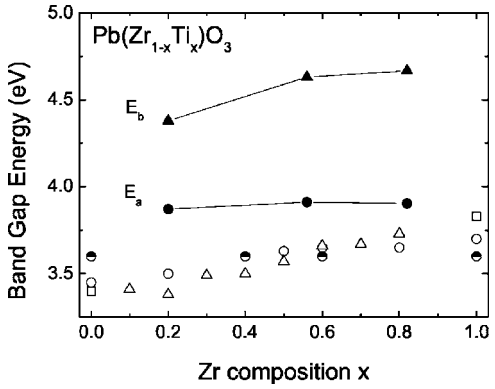

FIG. 4. Plot of bandgap values of PZTs (our own) and those from references. Filled symbols (our data of SE), symbols: unfilled circle (Ref. 2), unfilled triangle (Ref. 3), unfilled rectangle (Ref. 10), and half-filled circle (Ref. 4).

by about 0.15 eV. For example, the E_a energy values of PZT56 were 3.75 ± 0.02 and 3.91 ± 0.02 eV for the pyrochlore and perovskite phases, respectively. This result is consistent with the absorption data of Okada,[9] who showed that pyrochlore and perovskite of PZT52 have the optical bandgap energies of 3.76 and 4.20 eV, respectively.

In Fig. 4, we plotted the bandgap energy values as a function of Zr composition together with those from the literature.[2–4,10] With increasing Zr composition, the bandgap increased slightly for E_a and E_b, which is consistent with the literature. The slight increase or near-constancy of bandgap energies E_a and E_b of PZTs as a function of Zr content suggests that the substitution of Ti by Zr does not change much the electronic band structure of PZT materials. Our band-gap energy is about 0.1–0.4 eV larger than the literature values. For example, Peng and co-workers[2] estimated optical bandgap energies using absorption spectra. However, their values are smaller than our bandgap energies. The discrepancy may be due to the fact that the bandgap energies are determined accurately using SCP line-shape fitting in our work. Note that the optical bandgap values from literature were determined from the slope of optical absorption coefficient as a function of energy. This method is inaccurate and tends to underestimate the bandgap energy. We checked this by plotting absorption coefficient from our optical constant values. From the estimated refractive index values, we calculated the absorption coefficient. Note that complex refractive index $(n+ik)$ is the square root of dielectric function $(\varepsilon=\varepsilon_1+i\varepsilon_2)$. Using the absorption coefficient (α), we determined the optical band-gap values.[2,3] The fitted optical bandgap energy values were smaller by about 0.15 eV than E_a values; that is, the ellipsometrically determined values.

Robertson *et al.*[11] calculated the band structure of PZTs and showed a small increase of the fundamental bandgap energy with increasing Zr composition. They attributed the increase of the bandgap energy to the increase of X_1 conduction band energy due to a small change in lattice constant. Currently, electronic band structure calculations are in progress in order to compare to our experiments.

In summary, we measured pseudodielectric functions in the visible-ultraviolet spectral range of $Pb(Zr_xTi_{1-x})O_3$ $(x=0.2, 0.56,$ and $0.82)$ formed on platinized silicon substrates using sol-gel method and grown on (0001) sapphire by rf sputtering. Using both the POC and the SCP model methods, we estimated both the dielectric functions and the CP parameters of the PZT thin films. We found that the excitonic line-shape fitting produced the best fit to the data. The lowest energy peak near 4 eV is fitted as a double peak (E_a and E_b) for annealed PZTs due to the perovskite phase and as a single peak (E_a) for as-grown PZTs of mainly the pyrochlore phase. The CP energies of PZTs are consistent with literature values.

This work was supported in part by Office of Naval Research (Dr. C. E. C. Wood). H.L. was supported in part by Korea Research Foundation Grant No. KRF-2003-005-C00001. The authors are grateful to J. Evans at Radiant Technologies for providing data regarding the electrical characterization for PZT films.

[1] R. Ramesh, S. Aggarwal, and O. Auciello, Mater. Sci. Eng. **32**, 191 (2001), and references therein.
[2] C. H. Peng, J.-F. Chang, and S. B. Desu, Mater. Res. Soc. Symp. Proc. **243**, 21 (1992).
[3] S. Yang, D. Mo, and X. Tang, Ferroelectrics **287**, 35 (2003).
[4] M. P. Moret, M. A. C. Devillers, K. Wörhoff, and P. K. Larsen, J. Appl. Phys. **92**, 468 (2002).
[5] C. Millon, C. Malhaire, and D. Barbier, Sens. Actuators, A **113**, 376 (2004).
[6] D. E. Aspnes, Thin Solid Films **89**, 249 (1982).
[7] B. Johs, C. M. Herzinger, J. H. Dinan, A. Cornfeld, and J. D. Benson, Thin Solid Films **313/314**, 137 (1998).
[8] P. Lautenschlager, M. Garriga, L. Viña, and M. Cardona, Phys. Rev. B **36**, 4821 (1987), and references therein.
[9] A. Okada, J. Appl. Phys. **48**, 2905 (1977).
[10] V. I. Zametin, Phys. Status Solidi B **124**, 625 (1984).
[11] J. Robertson, W. L. Warren, and B. A. Tuttle, J. Appl. Phys. **77**, 3975 (1995).